Eur Phys J C **33**, s01, s503–s505 (2004)
Digital Object Identifier (DOI) 10.1140/epjcd/s2004-03-1675-x

EPJ C direct
electronic only

Exclusive vector meson production and DVCS at HERMES

R. Shanidze, on behalf of the HERMES collaboration

Physikalisches Institut, Universität Erlangen-Nürnberg, Germany

Received: 27 October 2003 / Accepted: 9 January 2004 /
Published Online: 17 February 2004 –

Abstract. The HERMES results from the hard exclusive processes such as ρ^o and ϕ meson production from hydrogen and Deeply Virtual Compton Scattering (DVCS) from different targets are presented. The data were collected in the scattering of the 27.6 GeV longitudinally polarized lepton beam of the HERA storage ring off an internal gas target. The measurement of the longitudinal cross-section σ_L for exclusive production of ρ^o and ϕ mesons and DVCS related beam-spin(A_{LU}), target-spin(A_{UL}), and beam-charge(A_C) azimuthal asymmetries in the single photon electroproduction process were found to be in agreement with theoretical predictions based on the GPD formalism.

PACS. 13.60.-f – 13.60.Le – 13.88.+e – 14.20.Dh – 24.85.+p

1 Introduction

The recent interest in hard exclusive processes is related to the formalism of Generalized Parton Distributions (GPD). In this formalism, which was introduced few years ago [1], the nucleon electromagnetic form factors and parton distribution functions(PDF) appear as limiting cases of the GPDs. Moreover, the orbital momentum contribution of the quarks and gluons to the nucleon spin, a quantity which can not be addressed in inclusive deeply inelastic scattering (DIS), can be accessed by the help of GPDs. Four different GPDs for each quark flavor q are necessary to parameterize the nucleon structure: $H^q(x,\xi,t)$, $E^q(x,\xi,t)$, $\tilde{H}^q(x,\xi,t)$ and $\tilde{E}^q(x,\xi,t)$. Here x is the Bjorken scaling variable, ξ (skewedness parameter) describes the difference in the quark longitudinal fractional momentum before and after interaction and t is the squared 4-momentum transfer between initial and final target states.

The simplest hard exclusive reactions are the production of a single particle in the lepton-nucleon scattering, which are described by so-called handbag diagrams. Two of these diagrams are shown in Fig. 1. The left panel of Fig. 1 corresponds to the single meson production process and the right panel represents the process of Deeply Virtual Compton Scattering (DVCS), in which a real photon is produced in a virtual photon-quark scattering. The hard scale in these processes is introduced by the incoming photon virtuality Q^2, which is equal to the squared four momentum transfer between the initial and the scattered leptons.

2 The HERMES experiment

The data have been collected by the HERMES experiment in the scattering of a 27.6 GeV longitudinally polarized electron (positron) beam of the HERA storage ring off an internal gas target. The beam polarization had an average value of 0.55 with a fractional uncertainty of 3.8%.

The scattered electrons and coincident particles in the selected events were measured by the HERMES spectrometer [2] in the polar-angle range of 40 to 220 mrad. The electrons were identified with an average efficiency of 98%, with a hadron contamination less than 1%. The angular resolution for the charged particles was better than 1 mrad and momentum was measured with a precision of about 2% . The hadrons were identified in the whole measured momentum interval by the dual-radiator RICH detector. The electromagnetic calorimeter, with an energy resolution of $\frac{\sigma_E}{E} = (5.1/\sqrt{E[GeV]} + 2.0) \cdot 10^{-2}$ was used for the photon measurements. The calorimeter provides an angular resolution for the photons of about 2 mrad.

The presented HERMES data were collected in the time period of HERA-I. They correspond to the integrated luminosity of about 1 fb^{-1} per nucleon, collected on polarized and unpolarized pure gaseous targets, including hydrogen, deuterium, neon and krypton. The comprehensive review of the HERMES results obtained in this running period can be found in [3].

3 Exclusive production of ρ^o and ϕ

The vector mesons ρ^o and ϕ were identified through their decays $\rho^o \to \pi^+\pi^-$ and $\phi \to K^+K^-$ by measuring the invariant masses $M_{\pi\pi}$ and M_{KK} respectively. The mass and the width of the reconstructed vector mesons ρ^o and ϕ were in good agreement with PDG values [4].

The exclusivity of the selected events with a scattered lepton and reconstructed ρ^o and ϕ was ensured by a cut in the excitation energy $\Delta E = \frac{M_X^2 - M^2}{2M} < 0.4$ GeV, where

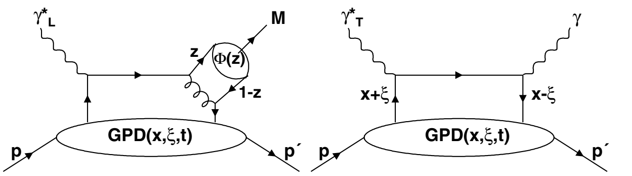

Fig. 1. The handbag diagrams for the hard exclusive processes: meson production (*left panel*) and DVCS (*right panel*)

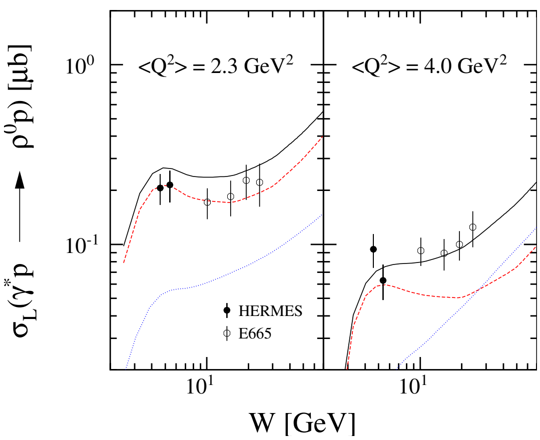

Fig. 2. The longitudinal component of the virtual-photoproduction cross section for ρ^0 production versus W at average Q^2 values of 2.3 (*left*) and 4.0 GeV^2 (*right*). The *solid lines* represent the results of the calculations of [7]. The *dashed (dotted) curves* represent the quark (two-gluon) exchange contributions within these calculations

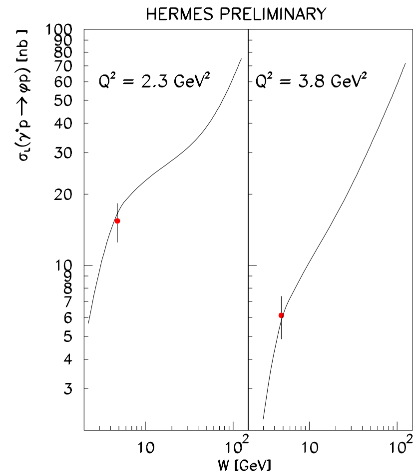

Fig. 3. The longitudinal component of the virtual-photoproduction cross section for ϕ production versus W at average Q^2 values of 2.3 (*left*) and 3.8 GeV^2 (*right*). The *solid lines* represent the results of gluon-exchange contribution only

M_X is the invariant mass of undetected particle(s) and M is the nucleon mass. The effect of the ΔE cut has been evaluated by a Monte Carlo simulation and corrections have been applied for the loss of exclusive events and for the background contributions. A detailed description of the exclusive ρ^o analysis at HERMES can be found in [5].

To compare the measurements with the GPD model calculations, the longitudinal cross-sections σ_L of exclusive ρ^o and ϕ production were extracted as a function of W, for two different intervals of Q^2. The invariant mass of the photon-nucleon system W was in the range 4-6 GeV and Q^2 varied from 0.7 to 5 GeV^2.

In Fig. 2 the results on σ_L for the exclusive ρ^o production from hydrogen are shown together with the calculations based on a GPD model [7]. The contributions due to quark exchange (dashed curves) and two-gluon exchange (dotted curves) are shown separately. On the same figure the results from E665 [6] are also shown. The data indicate that in the present kinematic domain the quark contributions dominate and only at $Q^2 = 4.0$ GeV^2 and W> 10 GeV the gluon exchange starts to contribute significantly. The agreement between the calculations and data is fairly good, in particular if one takes into account the existing theoretical uncertainties related to the size of the higher-twist contributions and the relatively low Q^2 values involved. The results obtained for ϕ are presented in Fig. 3. The solid curve in the figure represents only the contribution from two-gluon exchange. This mechanism is sufficient to describe the HERMES ϕ data, which indicates that the strange quark $s\bar{s}$ contribution in the nucleon at Q^2 probed by HERMES is almost negligible.

4 The DVCS measurements

DVCS is the cleanest process in which the GPDs can be measured. However, for the HERMES kinematical domain of relatively low Q^2, the main source of exclusive single photon events is the Bethe-Heitler (BH) process, where a photon is radiated by the incoming or scattered lepton. While it is impossible to distinguish between the BH and DVCS photons, the DVCS-BH interference can be exploited for the measurement of the DVCS amplitude. The interference term can be projected out by measuring azimuthal asymmetries in single photon electroproduction. It was shown that beam-spin (A_{LU}), target-spin(A_{UL}) and beam charge (A_C) azimuthal asymmetries provide access to the different combinations of the real and imaginary parts of the interfering amplitudes [8].

The DVCS related azimuthal asymmetries have been extracted from the HERMES single photon electroproduction events. These events were selected with an exclusivity cut $M_X < 1.7$ GeV, where the missing mass M_X was calculated as the invariant mass of the undetected particle(s). The selected exclusive sample, due to the finite M_X resolution, includes also non-exclusive background (mainly from $\pi^o \to \gamma\gamma$ decays) and contributions from nuclear resonances. These contributions have been taken into account by using Monte Carlo calculations. The description of the data selection and analysis for the measurement of the beam-spin azimuthal asymmetry A_{LU} on hydrogen can be found in [9], where for the average kinematic values $\langle Q^2\rangle$ =2.6 GeV ^{2}, $\langle x\rangle$ =0.11 and $\langle -t\rangle$ =0.27 GeV^2 the beam-spin analyzing power was measured as $A_{LU}^{\sin\phi}$=-0.23 $\pm$ 0.04 (stat) $\pm$ 0.03 (syst).

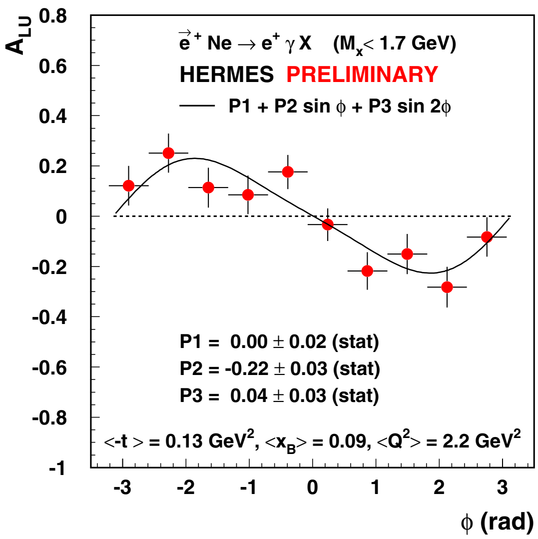

Fig. 4. The beam-spin azimuthal asymmetry $A_{LU}(\phi)$ measured from the neon target

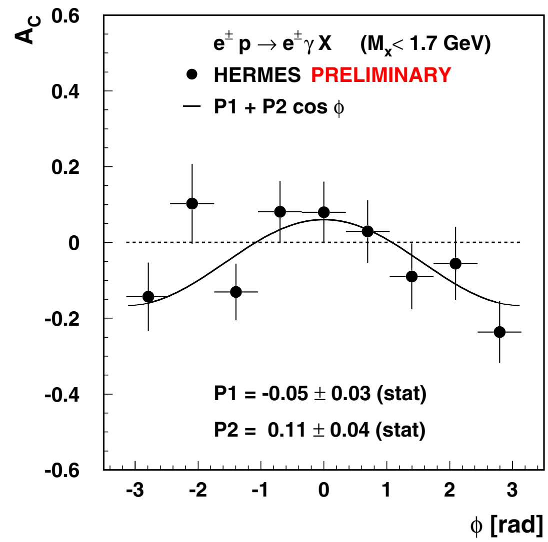

Fig. 5. The beam-charge azimuthal asymmetry $A_C(\phi)$ measured from the hydrogen target

The beam-spin azimuthal asymmetry A_{LU} was also measured from the other targets used by HERMES: deuterium, neon and krypton. Figure 4 shows $A_{LU}(\phi)$ measured from neon. The solid curve in the figure indicates the $\sin\phi$ behavior of $A_{LU}(\phi)$, in accordance with the expectations of the GPD formalism. In Table I the results on the beam-spin analyzing power $A_{LU}^{sin\phi}$ measured from hydrogen, deuterium, neon and krypton are presented. In the determination of the systematic error the instrumental effects (the HERMES acceptance and smearing) as well as the background and resonance contributions have been taken into account. In the presented results the contributions from coherent and incoherent processes on nuclei have not been separated. It should be noted that $A_{LU}^{sin\phi}$ on hydrogen in Table I is different from the value of [9], due to the different average kinematics of these measurements.

The longitudinal target-spin asymmetry A_{UL} was extracted for the deuterium target. The unpolarized beam sample was formed from the data samples with opposite beam polarizations. The average magnitude of the deuteron target polarization was 0.84, with a fractional systematic error of 4.4 %. The extracted value of the longitudinal target-spin azimuthal asymmetry, measured for $\langle Q^2\rangle$ =2.5 GeV ^{2}, $\langle x\rangle$ =0.10 and $\langle -t\rangle$ =0.18 GeV^2, was found to be $A_{UL}^{sin\phi} = -0.02 \pm 0.02(stat) \pm 0.01(syst)$.

Table 1. $A_{LU}^{sin\phi}$ from different targets

	$\langle Q^2\rangle$ GeV^2	$\langle x\rangle$	$\langle -t\rangle$ GeV^2	$A_{LU}^{sin\phi}$
H	2.5	0.12	0.18	-0.18±0.03±0.03
D	2.5	0.10	0.20	-0.15±0.03±0.03
Ne	2.2	0.09	0.13	-0.22±0.03±0.03
Kr	2.1	0.08	0.09	-0.17±0.07±0.03

The beam-charge asymmetry A_C, which is sensitive to the real part of the DVCS amplitude, was measured from the HERMES positron(e^+) and electron(e^-) data of single photon events on hydrogen. The luminosity averaged beam polarization of the total selected sample was close to zero. The extracted beam-charge azimuthal asymmetry A_C is shown in Fig. 5. The A_C data clearly indicate the expected $cos\phi$ dependence, with an amplitude 0.11 ± 0.04. The analyzing power for the beam-charge asymmetry, for the average kinematic values of $\langle Q^2\rangle$ =2.8 GeV^2, $\langle x\rangle$ =0.12 and $\langle -t\rangle$ =0.27 GeV^2, was found to be $A_C^{cos\phi} = 0.11 \pm 0.04(stat) \pm 0.03(syst)$.

5 Conclusion

The longitudinal cross section σ_L of the hard exclusive production of vector mesons ρ^o and ϕ from hydrogen and the DVCS related beam-spin, target-spin and beam-charge azimuthal asymmetries from different targets have been measured from the data collected by the HERMES experiment. These measurements were found to be in agreement with theoretical predictions based on the GPD formalism.

References

1. D. Müller et al.: Fortschr. Phys. **42**, 101 (1994); X. Ji: Phys. Rev. Lett. **78**, 610 (1997)
2. K. Ackerstaff et al.: Nucl. Inst. Meth. A **417**, 230 (1998)
3. K. Rith: Prog. Part. Nucl. Physics. **49**, 254 (2002)
4. K. Hagiwara et al.: Phys. Rev. D **66**, (2002)
5. A. Airapetian et al.: Eur. Phys. J. C **17**, 389 (1998)
6. M.R. Adams et al.: Z. Phys. C **74**, 237 (1997)
7. M. Vanderhaeghen et al.: Phys. Rev. D **60**, 094017 (1999)
8. M. Diel et al.: Phys. lett. B **411**, 192 (1997) A.V. Belitsky et al.: Nucl. Phys. B **629**, 323 (2002)
9. A. Airapetian et al.: Phys. Rev. lett. **87**, 182001 (2001)